Received: 30 May 2017 | Accepted: 22 August 2017

DOI: 10.1111/jace.15193

ORIGINAL ARTICLE

Journal of the American Ceramic Society

Cytotoxicity, chemical stability, and surface properties of ferroelectric ceramics for biomaterials

Matias Acosta[1] | **Rainer Detsch**[2] | **Alina Grünewald**[2] | **Virginia Rojas**[1] | **Jan Schultheiß**[1] | **Aleksandra Wajda**[3] | **Robert W. Stark**[4,5] | **Suman Narayan**[4,5] | **Maciej Sitarz**[3] | **Jurij Koruza**[1] | **Aldo R. Boccaccini**[2]

[1]Institute of Materials Science, Department of Geo- and Materials Science, Technische Universität Darmstadt, Darmstadt, Germany

[2]Institute of Biomaterials, Department of Materials Science and Engineering, Friedrich-Alexander-Universität Erlangen-Nürnberg, Erlangen, Germany

[3]Faculty of Materials Science and Ceramics, AGH University of Science and Technology, Cracow, Poland

[4]Physics of Surfaces, Institute of Materials Science, Technische Universität Darmstadt, Darmstadt, Germany

[5]Center of Smart Interfaces, Technische Universität Darmstadt, Darmstadt, Germany

Correspondence
Aldo R. Boccaccini, Institute of Biomaterials, Department of Materials Science and Engineering, Friedrich-Alexander-Universität Erlangen-Nürnberg Erlangen, Germany.
Email: aldo.boccaccini@ww.uni-erlangen.de
Jurij Koruza, Jurij Koruza, Institute of Materials Science, Department of Geo- and Materials Science, Technische Universität Darmstadt, Darmstadt, Germany.
Email: koruza@ceramics.tu-darmstadt.de

Funding information
Narodowe Centrum Nauki, Grant/Award Number: 2014/15/B/ST8/02827; Deutsche Forschungsgemeinschaft, Grant/Award Number: Leibniz program under RO954/22-1, KO 5100/1-1

Abstract

Surface chemistry and topo-physical properties determine the interactions of biomaterials with their physiological environment. Ferroelectrics hold great promise as the next generation of scaffolds for tissue repair since they feature tunable surface electrical charges, piezoelectricity, and sensing capabilities. We investigate the topography, wettability, chemical stability, and cytotoxicity in salient ferroelectric systems such as $(1-x)$ $(Na_{1/2}Bi_{1/2})TiO_3$–$xBaTiO_3$, $(1-x)Ba(Zr_{0.2}Ti_{0.8})O_3-x(Ba_{0.7}Ca_{0.3})TiO_3$, and $Pb(Zr,Ti)O_3$ to test their suitability as biomaterials. The lead-free ferroelectrics promote in vitro cell viability and proliferation to a considerably high extent. 0.94 mol % $(Na_{1/2}Bi_{1/2})TiO_3$–0.06 mol% $BaTiO_3$ showed the greatest potential leading to a cell viability of (149 ± 30)% and DNA synthesis of (299 ± 85)% in comparison to the reference. Lead leaching from $Pb(Zr,Ti)O_3$ negatively affected the cultured cells. Wettability and chemical stability are key factors that determine the cytotoxicity of ferroelectrics. These variables have to be considered in the design of novel electroactive scaffolds based on ferroelectric ceramics.

KEYWORDS

biocompatible materials, cytotoxicity, ferroelectrics, mouse embryonic fibroblasts, piezoelectric materials

1 | INTRODUCTION

Surface properties determine the adaptation of a biomaterial to the physiological environment and are thus essential for their proper function. Ferroelectrics are an important class of electroactive biomaterials, owing to their capability to interact with cells through electrical signals. Nonetheless, so far only a few works have addressed the interaction of different classes of ferroelectrics with physiological media. The interactions between the biomaterial surface and cells

determine, for example, morphology, proliferation, differentiation, and function. Variables such as surface chemistry, topography, wettability, and chemical stability have been traditionally considered as crucial parameters that determine cell expressions.[1-4] Thus, a careful analysis of these parameters is mandatory for the design of biomaterials.

Surface electrical charges in biomaterials have also been recognized as an important parameter that determines cell activity.[5-7] This is a result of cellular endogenous electrical and transmembrane voltage potentials.[8-12] For electroactive biomaterials, such as piezoelectrics, the terms "smart biomaterials"[9] or "the fourth generation of biomaterials"[10] have been coined. These materials feature the unique capability to interact with their physiological environment through electrical signals to foment tissue regeneration and sense cellular responses. As electroactive materials, ferroelectrics constitute a sub-class of piezoelectric materials.

Ferroelectrics are characterized by a spontaneous polarization that manifests as surface electrical charges. They feature extremely high piezoelectricity and sensing capabilities rendering that application of an electric field or mechanical load can be used for tuning their surface electrical charges. Thus, due to their surface electrical charges and piezoelectricity, they can interact with cells electrically or via nanoscale mechanical stimulation.[11-13] Ferroelectrics neither require external power sources to manifest surface electric charges, nor electrodes, which is a clear advantage over other electroactive materials.[11] Despite the enormous potential of ferroelectrics as novel "smart biomaterials," studies on their topo-physical properties, their chemistry, chemical stability, and cytotoxicity are still missing. This knowledge, however, is essential for theoretical and experimental works focusing on bioelectric signaling with ferroelectrics.

The most widely used ferroelectric material is Pb(Zr,Ti)O_3 (PZT), because of its superior piezoelectric properties and continuous engineering efforts over more than 5 decades.[14] Despite its outstanding electromechanical properties, major concerns regarding the toxicity of Pb[15-17] triggered the development of lead-free ferroelectrics.[18] Currently, the most thoroughly investigated lead-free ferroelectrics are $BaTiO_3$ (BT)-based, $(Na_{1/2}Bi_{1/2})TiO_3$ (NBT)-based, and $(K_{0.5}Na_{0.5})NbO_3$ (KNN)-based materials.[19] The $(1-x)(Na_{1/2}Bi_{1/2})TiO_3$–$xBaTiO_3$ (NBT–x mol% BT) is the most intensively investigated system from the NBT-based materials family since the discovery in 1991. It has high electromechanical properties and can be sintered at relatively low temperatures between 1100°C and 1200°C.[20] Although Bi is a heavy metal, studies in humans showed that this chemical element does not seem to have detrimental effects on human health.[21,22] The suitability of NBT-based compositions as biomaterials remains largely unknown. The $(1-x)Ba(Zr_{0.2}Ti_{0.8})O_3-x(Ba_{0.7}Ca_{0.3})TiO_3$ (BZT−x mol% BCT) is by far the most salient example from the family of BT-based materials due to its outstanding piezoelectricity.[23] Very recent works highlighted the potential applicability of BZT-BCT as biocompatible nanogenerators[24] and thin films,[25] albeit no investigation of topo-physical features and chemical stability has been done. Several KNN-based materials with remarkable piezoelectric properties have also been reported,[26] although their processing remains challenging[27] and cytotoxicity of several compositions did not reveal promising results.[28,29]

Taking into account the perspectives on the development of ferroelectrics as electroactive biomaterials, we investigate topography, wettability, chemical stability, and cytotoxicity of salient ferroelectric systems. We focus our experiments on NBT–6BT, BZT–60BCT, and PZT. We selected the lead-free compositions because their d_{33} values are similar. We contrast these results with PZT in order to get insights into the cytotoxicity caused by lead in classical piezoelectric ceramics. We demonstrate that lead-free ferroelectrics hold great promise as biomaterials because they promote mouse embryonic fibroblast (MEF) activity and DNA synthesis to a considerably high extent.

2 | EXPERIMENTAL PROCEDURE

2.1 | Materials

Three ferroelectric materials were selected for this investigation based on their technological relevance. Namely, the 0.94 $(Na_{1/2}\ Bi_{1/2})TiO_3$–$0.06BaTiO_3$, $0.40Ba(Zr_{0.2}Ti_{0.8})O_3$–$0.60(Ba_{0.7}Ca_{0.3})TiO_3$, and commercially available soft PZT PIC 151 (PI Ceramic GmbH, Germany). The lead-free ferroelectrics were synthesized via a solid state mixed oxide route with raw chemicals from Alfa Aesar (Alfa Aesar GmbH & Co., Karlsruhe, Germany). The raw chemicals Bi_2O_3 (purity 99.975%), Na_2O_3 (purity 99.5%), TiO_2 (purity 99.6%), $BaCO_3$ (purity 99.8%), $CaCO_3$ (purity 99.5%), and ZrO_2 (purity 99.5%) were mixed according to the respective stoichiometry. The synthesis procedure of NBT–6BT calcined powders is described elsewhere.[30] Calcination was done at 800°C for 3 hours, with a heating rate of 5°C/min. The processing details for the BZT-60BCT powders can be found elsewhere.[31] Calcination was done at 1300°C for 2 hours. Calcined powders of both systems were pressed into green bodies of 40 g with dimensions of (70 × 40 × 5) mm^3. The procedure to compact such specimens has been described previously.[32] While no binder was used for NBT–6BT, 2 g of binder (5 wt% Polyvinyl butyral and 95 wt% ethanol) were required for the green bodies of BZT–60BCT. Green bodies of NBT–6BT were initially shaped using 53 MPa uniaxial pressure for 10 minutes (type 2SPW25, Walter Neff Maschinenbau, Karlsruhe, Germany), whereas for BZT–60BCT the initial shape was done using 6 MPa uniaxial

pressure during 10 minutes (type 2SPW25, Walter Neff Maschinenbau, Karlsruhe, Germany). After the initial shaping, cold isostatic pressing at 300 MPa for 1.5 minutes was applied to the green bodies of both systems (KIP 100 E, Paul-Otto Weber GmbH, Germany). Sintering of NBT–6BT green bodies was done at 1100°C for 3 hours with a heating rate of 5°C/min. For BZT–60BCT, the binder was burned out at 600°C for 3 hours, with a heating rate of 0.5°C/min. Thereafter, sintering was done at 1500°C for 2 hours with a heating rate of 5°C/min. Following this procedure, all synthesized samples showed relative densities above 95% and grain size and morphology as described elsewhere.[30,31]

Several disc-shaped samples of 0.5 mm thickness and 10 mm diameter were drilled from each material system. After the drilling process, all specimens were ground using a semiautomatic grinding station with a diamond coated (15 μm diameter) grinding wheel (ZB 42T, Ziersch Fertigungstechnik GmbH & Co. KG, Germany). Thereafter, all samples were cleaned in acetone in an ultrasonic bath. Afterward, all samples were annealed at 400°C to remove residual stresses that were induced by the grinding process.

2.2 | Surface topography

The nano-roughness of the samples was studied using a Nanowizard 3 Bioscience (JPK Instruments AG, Germany). PPP-ZEIHR cantilevers (Nanosensors, NanoWorld AG, Germany) with a resonance frequency of about 130 kHz and a force constant of about 20 N/m were used to scan the sample surfaces. Three identical samples were scanned at three different points each. Mean values and standard deviation were calculated from these data. The investigated area was (1.5 × 1.5) μm² with a scanning rate of 0.4 Hz. The roughness parameters R_a (average roughness) and R_{rms} (root mean square roughness) were calculated according to the standard JIS B 0601: 1994. Micro-roughness was also characterized in all samples. No substantial differences between the samples roughness was measured, thus we do not discuss details on these measurements here.

2.3 | Wettability

The wettability of the piezoceramics was studied by means of static contact angle (CA) measurements (OCA 20, Dataphysics Instruments GmbH, Germany). A droplet of 2 μL deionized water (resistivity 18.2 MΩ·cm) was placed on the surface and the CA was derived using Youngs-Laplace fitting to the drop shape. The mean value of the water CA was obtained from at least five droplets on each sample.

The surface energy (SE) of the piezoceramics was determined using three test liquids namely, water, diiodomethane and ethylene glycol at room temperature. The surface energy value was calculated according to Owens, Wendt, Rabel and Kaelble (OWRK) method which gives both the disperse ($SE_{disperse}$) and the polar part (SE_{polar}) of the surface energy.

2.4 | Chemical stability

Prior to the chemical analysis of leaching ions in simulated body fluid (SBF), the samples were sterilized at 100°C. The concentration of the relevant cations for this work in SBF (following indications as described in the next paragraph) were 94.2 mmol·L^{-1} Na^+, 3.84 mmol·L^{-1} K^+, 1.18 mmol·L^{-1} Mg^{2+}, and 1.88 mmol·L^{-1} Ca^{2+}. The pH value of the SBF prior to soaking experiments was 7.40. Immersion in SBF was done at 37°C for times of 1 hour (0.042 days), 24 hours (1 day), 240 hours (10 days), and 720 hours (30 days) using a ratio of 0.2 g sample to 20 mL of solution.

The resulting solutions with leached ions were then analyzed directly using an inductively coupled plasma mass spectrometer (ICP-MS) (6100 Perkin Elmer PerkinElmer Inc., United States) with a detection limit between 0.01 μg/L and 100 g/L as well as with an inductively coupled plasma optical emission spectrometer (ICP-OES) (Plasm 40 Perkin Elmer, PerkinElmer Inc., United States) with detection limit between 1 μg/L and 1000 g/L. ICP-MS was chosen for Ba, Bi, Pb, Ti, and Zr ions because of their very low concentration in the SBF, whereas ICP-OES was used to detect Ca and Na cations because of their high concentration as consequence of their inherent presence in the SBF. The concentration of ions in SBF was also measured for reference. All the ICP measurements were performed in an accredited laboratory following the standards PN-EN ISO 11885:2009 for ICP-OES and PN-EN ISO 17294-2:2006 for ICP-MS. For statistical purposes, measurements were performed on three different samples for each soaking time. The results are reported in the form of a mean value and standard deviation.

2.5 | Cytotoxicity

Mouse embryonic fibroblast (MEF) cells were used to assess the cell-surface interactions, as described elsewhere.[33] MEF cells were seeded at a density of 100 000 cells/sample, cultured in Dulbecco's modified Eagle's medium (DMEM) (Gibco®, Thermo Fisher Scientific GmbH, Germany) supplemented with 10% (v/v) fetal calf serum (FCS) (Sigma-Aldrich GmbH, Germany) and 1% (v/v) antibiotic-antimycotic (Gibco®, Germany) and incubated in a humidified atmosphere of 95% relative humidity and 5% CO_2, 37°C.

After an incubation period of 24 hours, MEF cells were analyzed for cell proliferation by quantifying the amount of DNA synthesis, cell activity by assessing cell viability and cell morphology by scanning electron microscopy (SEM)

(Auriga CrossBeam, Carl Zeiss Microscopy GmbH, Germany). The 5-bromo-2′-deoxyuridine (BrdU) assay (Roche Diagnostics GmbH, Germany) is based on the detection of BrdU incorporation into genomic DNA of proliferating cells. Following incorporation, BrdU was then colorimetrically detected by an ELISA reader (Phomo, Anthos Mikrosysteme GmbH, Germany).

The viability of seeded MEFs on the samples was assessed through the enzymatic conversion of tetrazolium salt (WST-8 assay kit, Sigma-Aldrich GmbH, Germany) after 24 hours of cultivation. Culture media was completely removed from the incubated films and subsequently added 1% (v/v) WST-8 assay kit containing culture medium and incubated for 2 hours. 100 μL of supernatant from each sample was transferred into a well of a 96 well-plate and measured the absorbance at 450 nm with a microplate reader (PHOmo, Autobio Labtec Instruments co. Ltd., China).

For the SEM investigation, the MEF cells were fixed with a solution containing 3% (v/v) glutaraldehyde (Sigma-Aldrich GmbH, Germany) and 3% (v/v) paraformaldehyde (Sigma-Aldrich GmbH, Germany) in 0.2 $mol \cdot L^{-1}$ sodium cacodylate buffer (pH 7.4) and rinsed three times with phosphate-buffered saline (PBS) solution. In a next step, the samples were incubated in a diluted ethanol series starting from a concentration of 30% up to 99.8%. Afterward, the samples were critical point dried (EM CPD300, Leica Camera AG, Germany) and analyzed in SEM (Auriga CrossBeam, Carl Zeiss Microscopy GmbH, Germany).

2.5.1 | Statistics

For the cell viability studies, the results are presented using the mean value and standard deviation of four replicates of each sample type. All results were normalized to cell growth on the cell culture well-plate surface (REF = 100%). The differences in analysis parameters between the different samples investigated were evaluated by one-way analysis of variance (ANOVA). The level of the statistical significance was defined at $P < .05$ (Origin 8.1G, Origin Lab Corporations, USA). The significance level was set as $P < .05$: not significant, $P < .01$: significant, and $P < .001$: highly significant. The Turkey test was used for comparing the mean values.

3 | RESULTS

3.1 | Surface topography

Figure 1A-C show the topographies obtained by atomic force microscopy (AFM) for NBT–6BT, BZT–60BCT, and PZT, respectively. The sample surfaces were ground by a semiautomatic grinding station. The grinding procedure caused characteristic micro-roughness for all samples with regular changes in topography in the range between 10 μm and 20 μm (not shown). This micron-size topography is not expected to alter cell adhesion, spreading, or activity to a great extent.[34] Thus, we focus further on the investigation of the nano-roughness that has been generally recognized as a major factor determining the cell activity.[4]

Figure 1 also shows the nano-roughness parameters used for the topography characterization that includes the average roughness (R_a) and root mean square roughness (R_{rms}). The average roughness values are all within the same order of magnitude. The slight deviations between the samples topographies can be attributed to their different hardness.[35,36] The root mean square roughness indicates little variations between the lead-free ferroelectrics (Figure 1A-B), although PZT has a slightly lower root mean square roughness.

3.2 | Wettability

The contact angle (CA) of water at room temperature was used to determine the wettability of the ferroelectric materials. The CA of water on NBT–6BT, BZT–60BZT, and PZT surfaces is displayed in Figure 2A-C, respectively. Despite the minor differences in the surface topography, the three system surfaces showed a clear difference in their wettability.

The lead-free ferroelectrics have a hydrophilic nature. The NBT–6BT is the most hydrophilic system with a CA = (59 ± 8)°. The BZT–60BCT is also hydrophilic and has CA = (87 ± 4)°. Considering the high CA of BZT–60BCT and the measurement uncertainty, it is clear that this material is quite close to being hydrophobic. PZT is the only clear hydrophobic system, as indicated by a CA = (104 ± 4)°.

The SE measurements indicated that NBT–6BT had the highest SE value of 52 mJ/m^2 with $SE_{disperse}$ = 40.09 mJ/m^2 and SE_{polar} = 11.69 mJ/m^2. The BZT–60BCT exhibited a SE of 46.2 mJ/m^2, where the $SE_{disperse}$ = 44.91 mJ/m^2 and SE_{polar} = 1.25 mJ/m^2. The PZT had the lowest SE value of 42.72 mJ/m^2 with $SE_{polar} \approx 0$.

3.3 | Chemical stability

Figure 3 introduces the results of the chemical stability experiment performed for all systems in SBF at 37°C. Figure 3A presents the ion dissolution of Ba and Pb cations as a function of soaking time. Due to the relatively low concentration of these cations in SBF, the measurements were performed by means of ICP-MS. After 30 days of soaking time the concentrations of Bi, Ti, and Zr cations in the SBF were below the detection limit of the instrument. Thus, considering the detection limit of our experimental setup of 0.01 μg/L, we can assure a considerably low or even negligible leaching of Bi, Ti, and Zr cations.

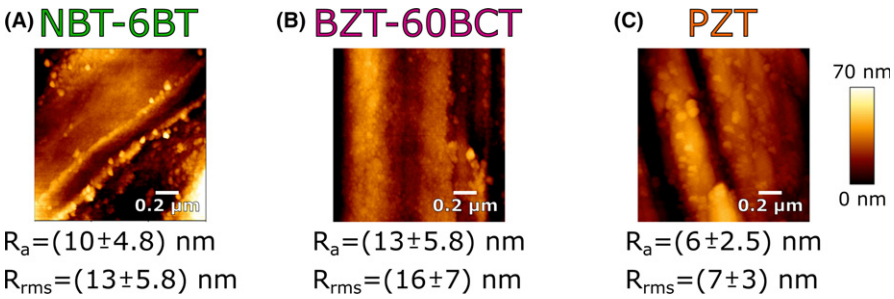

FIGURE 1 Sample surfaces and roughness parameters measured by AFM for (A) NBT–6BT, (B) BZT–60BCT, and (C) PZT [Color figure can be viewed at wileyonlinelibrary.com]

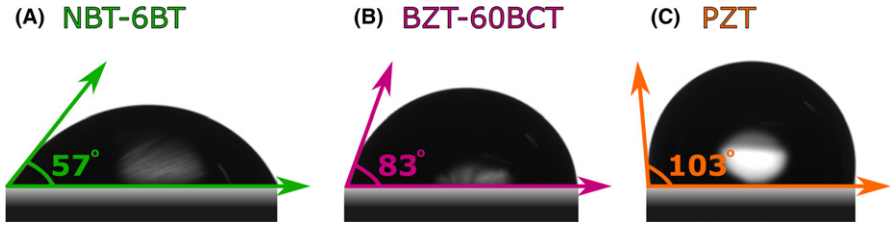

FIGURE 2 Pictures of the CA of water on (A) NBT–6BT, (B) BZT–60BCT, and (C) PZT [Color figure can be viewed at wileyonlinelibrary.com]

Figure 3B displays the concentration of the Na and Ca cations as a function of soaking time, measured with ICP-OES. This technique was used because of the high concentration of these cations in the SBF. All cations increase their concentration exponentially with increasing soaking time, although Ba leached from BZT–60BCT and Pb leached from PZT seem to saturate after 10 days of soaking time.

From the detectable cations with low concentration (Figure 3A), it is seen that Ba increases its concentration more rapidly than Pb. The BZT–60BCT has a higher concentration of Ba so this cation increases its concentration in the leached SBF one order of magnitude more than in the case of NBT–6BT. Pb is also leaching with a detectable concentration even after 1 day of soaking time. Despite the high content of Na and Ca in the SBF, there is still a driving force that leads to leaching of Na and Ca into the SBF. The chemical instability of ferroelectrics influences cells adhesion and proliferation, as will be discussed in Section 4.

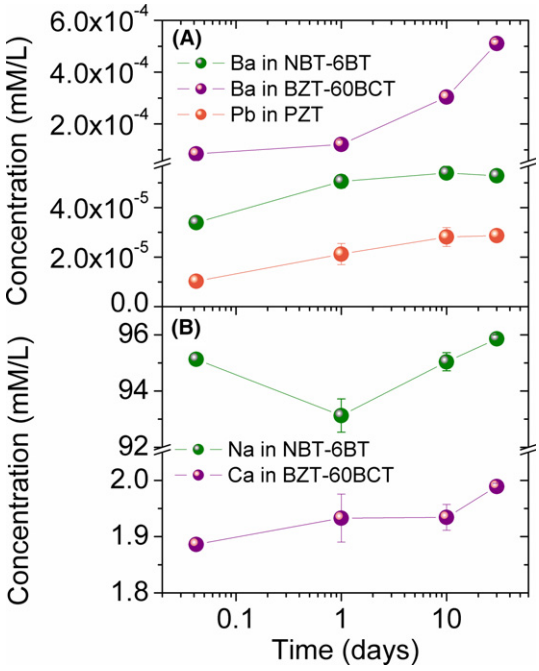

FIGURE 3 Leaching experiment in SBF. (A) Cation concentration measured by means of ICP-MS. (B) Cation concentration measured by means of ICP-OES. Note that Bi, Ti, and Zr cations are not present in the figures because their concentration remained below the detection limit of the measurements even after 30 days of soaking time [Color figure can be viewed at wileyonlinelibrary.com]

3.4 | Cytotoxicity

The activity of MEF is a conclusive test to evaluate the cytotoxicity of biomaterials.[37] Figure 4 displays the MEF viability and proliferation results obtained after 24 hours of cultivation. The results were normalized to the cell growth on a Petri dish. The significance level for the results is indicated by the symbol "*" within the figure and was set as $*P < .05$: not significant, $**P < .01$: significant, and $***P < .001$: highly significant. Both lead-free ferroelectrics induced a considerable enhancement of cell viability with the results being statistically highly significant, as pointed out in Figure 4. This is indicated by the high cell viability of (149 ± 30)% in the cells cultivated on NBT–6BT, as well as in BZT–60BZT with a cell viability of (138 ± 35)%. In contrast, PZT did not enhance cell viability since we measured a value of (98 ± 14)% compared to the reference.

The proliferation of MEF cells indicated by their DNA synthesis revealed the same trends as the viability tests. Both lead-free ferroelectrics induced a considerably high

DNA synthesis, with an enhancement of (299 ± 85)% in NBT–6BT and of (310 ± 80)% in BZT–60BZT as compared to the reference. For PZT, the DNA synthesis activity in MEF cells was much lower. A DNA synthesis of (115 ± 25)% was measured for PZT as compared to the reference. The results give a substantial indication of the biocompatibility of the investigated lead-free ferroelectrics.

Figure 5 shows SEM micrographs for (A), (D) NBT–6BT; (B), (E) BZT–60BCT; and (C), (F) PZT surfaces after 24 hours of MEF incubation. The MEF cells almost completely cover the surface of the NBT–6BT and form a multilayer structure (Figure 5A), thus it was not possible to analyze single cells. The overall morphology of the cell multilayer indicated a preferred growth orientation.

The cell density on BZT–60BCT (Figure 5B,E) was lower than on NBT–6BT. The MEF cells spread quite considerably but did not completely cover the materials' surface (Figure 5B). Single cells could be detected with the presence of filopodia or very thin extensions. Very recently similar results have been reported for BZT–45BCT thin films.[25] Even in the case of PZT (Figure 5C,F), MEF cells spread extensively, although they covered a much smaller surface area in comparison to the other samples. The MEF cells on PZT were also much more flattened than in lead-free ferroelectrics. In this case, single cells characterized by a polygonal shape with filopodia or very thin extensions were easily distinguishable. For BZT–60BCT and PZT, we did not discern preferred growth orientation of the MEF cells.

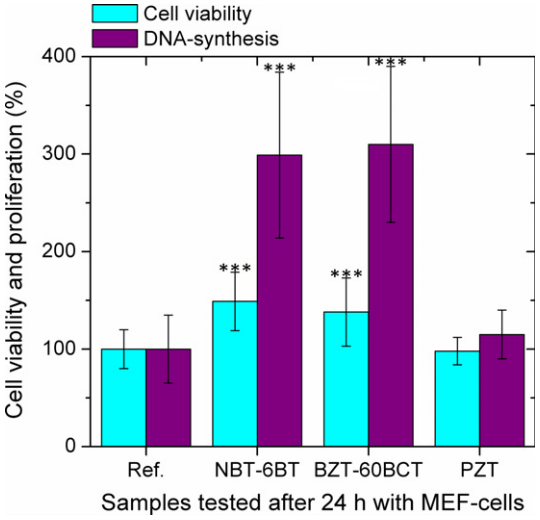

FIGURE 4 Cell viability and proliferation of MEF cells on REF, NBT–6BT, BZT–60BCT, and PZT after 24 h of cultivation, normalized to cell growth on Petri dishes.[37] ***$P < .001$: highly significant [Color figure can be viewed at wileyonlinelibrary.com]

4 | DISCUSSION

The cytotoxicity results indicate that that NBT–6BT offers the best cell viability of (149 ± 30)%, followed closely by the cell viability of BZT–60BCT with (138 ± 35)%. The DNA synthesis of cells on NBT–6BT was (299 ± 85)%, which is quite similar to the DNA synthesis of the cells on BZT–60BZT with (310 ± 80)%. In contrast, cells on PZT feature a much lower cell viability of (98 ± 14)% and DNA synthesis of (115 ± 25)%.

The nano-roughness did not differ much between the samples. Considering the measurement errors, no relevant discrepancies were found for the R_a values. PZT, however, did show smaller R_{rms} values than lead-free ferroelectrics. The higher discrepancy between R_{rms} values than between R_a values can be explained considering the calculation of both roughness parameters. From a mathematical point of view, R_a assigns equal statistical weight to each roughness measurement. In contrast, the R_{rms} emphasizes the extreme roughness values due to the square terms involved in its calculation. The extremes of the nano-roughness measurements of our samples tend to be in the order of microns. Thus, they are directly linked to the grinding process. Since this micron-size topography is not expected to affect cell behavior considerably,[34] we will neglect the effect of surface roughness in further discussion. We further justify this approximation taking into account that a previous work indicated that, in materials with similar nano-roughness, rat osteoblasts adhesion, spreading, proliferation and differentiation were determined by the wetting characteristics rather than nano-topography.[8] In other words, under similar nano-roughness, we expect that the wettability and chemical stability influence more considerably the cell viability and proliferation. We also note that due to the high and similar Young's moduli of perovskite ferroelectric ceramics,[14] we do not expect that elasticity plays a major role.

In materials with hydrophobic surfaces, cell adhesion and spreading are generally limited. In contrast, moderately hydrophilic or hydrophilic surfaces tend to favor cell adhesion and spreading.[4,38-40] This was shown exemplary on surface-treated polymers with human fibroblasts, human MG63 osteosarcoma cells, Chinese hamster ovary, Chinese hamster fibroblast, and Chinese hamster endothelial cells.[38-40] NBT–6BT is the most hydrophilic material investigated here with a CA = (59 ± 7.6)°. This CA is in the same range that was previously highlighted to maximize cell adhesion and proliferation.[39] This maximization of cell adhesion and spreading can be reconciled taking into account that moderately hydrophilic surfaces with CA between 60° and 65° maximize the adsorption of cell-adhesive proteins.[41] The other lead-free ferroelectric, BZT–60BCT, features a CA = (87 ± 4)° which is in the limit of

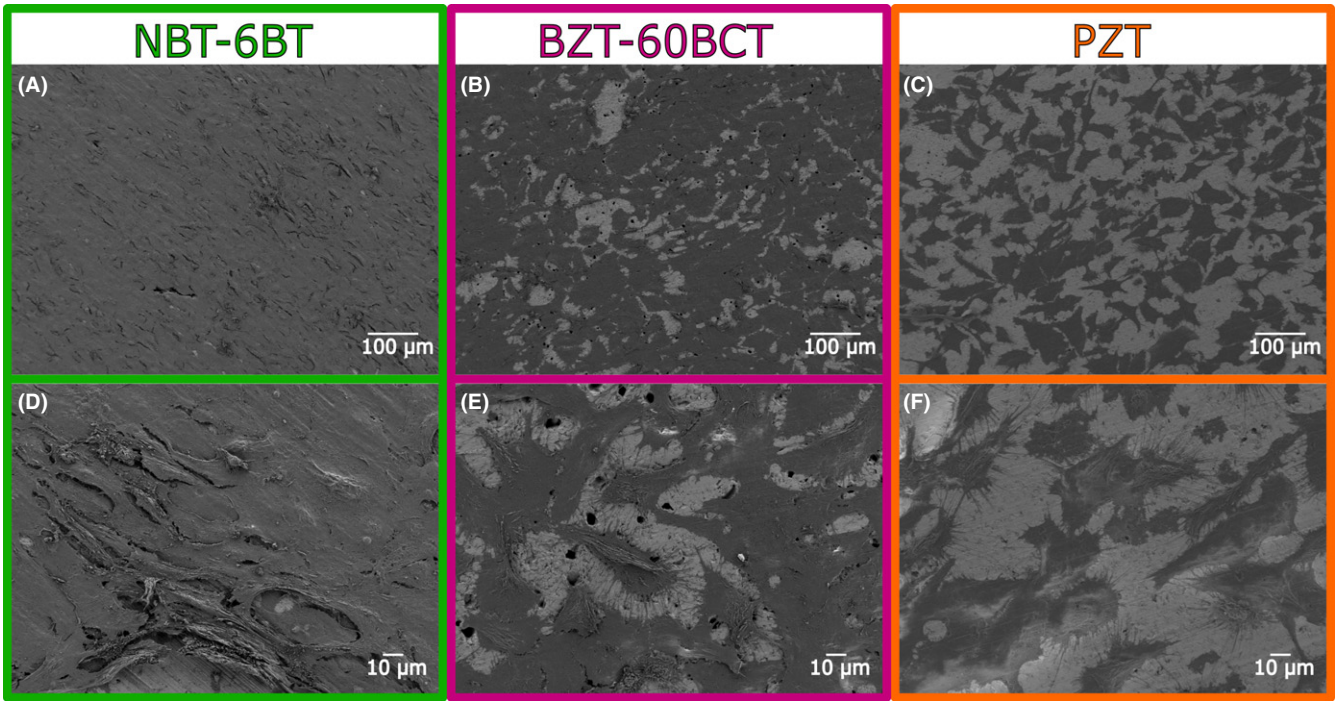

FIGURE 5 SEM-images of MEF cells on as-polished surface of NBT–6BT (A) and (D), BZT–60BCT (B) and (E), and PZT (C) and (F) after 24 h of incubation. (D-F) are images with higher magnification on the same material but from a different area [Color figure can be viewed at wileyonlinelibrary.com]

hydrophobic surfaces. PZT has a hydrophobic surface with CA = (104 ± 4)°. Therefore, wettability seems to be a major factor determining the cell activity and proliferation. However, the effect of the surface chemistry must also be taken into account,[40] especially considering that ions leach from the perovskite ferroelectric ceramics into aqueous environments as shown in Figure 3 and in the literature.[28,29,42-44]

The chemical stability of surfaces in contact with biological media is extremely important since it can affect the cell activity and proliferation.[1,3,4,45] Our experiments with commercial PZT (PIC 151) indicate that the material is unstable in aqueous media. Figure 3 highlights that Pb is the most leachable species of PIC 151 and other cations of this material remain below the detection limit of our device. Similar results were obtained for other PZT-based materials .[42-44] Pb leaching rates depend on the chemical composition of the material, sintering conditions, as well as the composition and pH value of the aqueous media.[42-44] This is a major concern for technological applications in contact with aqueous media or under atmosphere conditions such as ferroelectric ceramics implemented as biomaterials, sensors or actuators. It is also a concern in other applications for which lead-containing ceramics are currently under investigation such as perovskite solar cells.[46,47]

Mitochondrial dysfunction can be interpreted as a cytotoxicity measure due to the crucial role of this organelle in maintaining the cellular structure and function. Thus, it directly affects the cell viability.[48] Reduction of 50% in cell viability as compared to the reference can be well attributed to cytotoxicity.[49] We did not observe such a dramatic reduction of MEF cell viability on the cells cultivated 24 hours on PZT. We attribute this to the limited leaching of Pb to the SBF after 24 hours (Figure 4) since MEF cells generally display a quasi-instantaneous reactivity to their environment.[33] Despite that there is no clear cytotoxicity, the negative effect of Pb leached ions is corroborated taking into account the much lower cell density observed on PZT as compared to the lead-free ferroelectrics (Figure 5). Experiments with Chinese hamsters and mouse fibroblasts also indicated relatively low cell density and proliferation on PZT surfaces even after longer periods of incubation.[50,51] Moreover, it was also demonstrated that a considerable fraction of mouse fibroblasts has survival time shorter than 4 days on PZT.[51]

Overall the cells on the lead-free ferroelectrics show good adhesion, spreading, and mutual interconnections (Figure 5). On NBT–6BT even a MEF multilayer structure formed covering the complete materials' surface with a preferred growth orientation. Together with the high MEF cell activity and DNA synthesis, this implies that the material can be considered as a promising biomaterial. At this point, it is worth analyzing the potential human toxicity of other transition metals.[52] To date, Bi does not seem to show detrimental effects to human health.[21,22] Nonetheless, it should be pinpointed that cytotoxicity of the $Bi(NO_3)_3$ salt was

demonstrated for a concentration higher than 1.20×10^{-2} mmol·L^{-1} after testing the viability of murine fibroblasts L929 and murine osteoblastic cells MC3T3-E1.[52] The results of our ICP analysis indicate that Bi concentration in the SBF remains below 0.01 μg/L even after 30 days of soaking time of NBT–6BT. Thus, at this concentration doses, Bi does not affect cells activity or proliferation.

Ba is present in NBT–6BT and in BZT–60BCT. For both materials, we could detect leaching of Ba into the SBF. The concentration of Ba in the SBF was much higher for BZT–60BCT than for NBT–6BT, which is expected due to the much higher content of Ba in the former material. This alkali earth metal is characterized by a low cytotoxicity as corroborated by a study on the effect of $BaCl_2$ salt in the viability of murine fibroblasts L929 and murine osteoblastic cells MC3T3-E1. This work determined that a concentration higher than 1.26×10^{-03} mol/L leads to cytotoxicity.[52] Moreover, no clear beneficial physiological effects were reported so far for Ba cations.[53] Thus, we do not expect that Ba is playing a major role in determining the cell viability or proliferation here. We note, however, that some studies on animals indicated that Ba could be incorporated into the bone matrix replacing Ca albeit no detrimental effects on the bone integrity were reported.[54]

Na and Ca are present in bioactive glasses and are expected to have a positive physiological effect.[45,53] Some of their positive effects can include favoring human osteoblast proliferation, differentiation, and extracellular matrix mineralization. We speculate that the high leaching rate and concentration of Na in NBT–6BT could actually favor the cellular proliferation more positively than the much lower Ca leaching rate of BZT–60BCT. More detailed experiments are required to verify this hypothesis. The correlation between the wettability and cytotoxicity for the investigated materials, makes us believe that wettability might be the major factor affecting cell viability, adhesion, and proliferation.

Another important aspect that affects cell activity and proliferation is the surface electrical charge. The surface topography, chemical composition, and crystal structure determine the wettability, surface energy, and surface electrical charges. For instance, the effect of the surface charges on the CA was demonstrated for differently polarized hydroxyapatite.[55] Moreover, also for hydroxyapatite, it was shown that surface energy and electrical charges have a mutual interdependence.[56] Therefore, the wettability, surface energy, and surface electrical charges are clearly interdependent in electroactive materials.

From the results presented in Figure 1, it follows that we may safely neglect the effect of the topography in the context discussed here. Moreover, all the materials in this work have a perovskite crystal structure. Thus, in the lead-free ferroelectrics investigated here, the key parameters responsible for the wettability are the surface energy (SE) and electrical charges. Since the materials have not been poled, no net macroscopic polarization should be expected. However, on the local cell level, electrical charges are certainly present as consequence of the characteristic spontaneous polarization of ferroelectrics. On a local scale, the grain crystallographic orientation is responsible for determining the spontaneous polarization and thus also the surface electrical charges of ferroelectrics. This, in turn, affects the wettability. In this study, we annealed all samples to avoid the influence of ferroelastically induced domain texturing that could result from residual stresses. The measurements of SE indicated that NBT–6BT had the highest SE_{polar} with a value of 11.69 mJ/m^2. The SE_{polar} of the BZT–60BCT and PZT were 1.25 mJ/m^2 and almost 0, respectively. This means that NBT–6BT has highest polar interactions available as compared to other samples with little polar interactions. Thus, electrowetting could be the reason behind the tendency found on the wettability of the systems. Namely, NBT–6BT is the most hydrophilic material, whereas PZT is the most hydrophobic one. The surface electrical charges and thus the hydrophilic nature of the NBT–6BT seem to have a positive effect on cell adhesion and proliferation.[57,58]

5 | CONCLUSIONS

In this work, we discuss the potential of ferroelectric materials as biomaterials. We contrast lead-containing and lead-free ferroelectrics. $Pb(Zr,Ti)O_3$ (PIC 151), which is a commercially relevant lead-based ferroelectric, was chosen as representative lead-containing material. Two promising lead-free ferroelectrics, $0.94(Bi_{1/2}Na_{1/2})TiO_3$–$0.06BaTiO_3$ and $0.40Ba(Zr_{0.2}Ti_{0.8})O_3$–$0.60(Ba_{0.7}Ca_{0.3})TiO_3$, were selected as lead-free representative materials. We investigated the cell growth, proliferation, and viability. Among the three materials, $0.94(Bi_{1/2}Na_{1/2})TiO_3$–$0.06BaTiO_3$ showed the best performance since it promotes a high cell viability of (149 ± 30)% and DNA synthesis of (299 ± 85)% with respect to the reference.

The materials were characterized in terms of chemical stability, wettability, and surface roughness. All three ferroelectrics were chemically unstable in SBF, with the A-site cations Pb, Na, Ba, or Ca being the only detectable species leaching after 30 days of immersion. Taking into account the cytotoxicity of lead, it is evident that $Pb(Zr,Ti)O_3$ should not be used in applications as a biomaterial or under environmental conditions. Despite this effect, our results highlight that the wetting angle and thus surface energy determine the biocompatibility of the ferroelectrics. $0.94(Bi_{1/2}Na_{1/2})TiO_3$–$0.06BaTiO_3$ is moderately hydrophilic with a contact angle of (59 ± 8)° and has the highest polar

surface energy of 11.69 mJ/m^2, while both other materials were hydrophobic and featured lower polar interactions.

Our results indicate that the complexity of the interaction of ferroelectrics and piezoelectrics with a physiological environment call for a better understanding before these materials can be used in biomedical applications. Corroborating the evolution of primary cells and/or target cells on ferroelectrics is certainly required. Further work towards ferroelectric biomaterials can also focus on the modification of surface energy, surface electrical charges, and wettability through poling (ferroelectricity) or mechanical loading (piezoelectricity).

ACKNOWLEDGMENTS

MA acknowledges the support of the Leibniz program under RO954/22-1. JK and JS acknowledge the support of the Deutsche Forschungsgemeinschaft (DFG), Grant Nr. KO 5100/1-1. AW and MS acknowledge the support of the National Science Centre Poland under project 2014/15/B/ST8/02827.

ORCID

Matias Acosta http://orcid.org/0000-0001-9504-883X
Virginia Rojas http://orcid.org/0000-0003-2283-229X
Robert W. Stark http://orcid.org/0000-0001-8678-8449
Jurij Koruza http://orcid.org/0000-0002-0258-6709
Aldo R. Boccaccini http://orcid.org/0000-0002-7377-2955

REFERENCES

1. Ozdemir T, Higgins AM, Brown JL. Osteoinductive biomaterial geometries for bone regenerative engineering. *Curr Pharm Des*. 2013;19:1-10.
2. Menzies KL, Jones L. The impact of contact angle on the biocompatibility of biomaterials. *Optom Vis Sci*. 2010;87:387-399.
3. von der Mark K, Park J. Engineering biocompatible implant surfaces. *Prog Mater Sci*. 2013;58:327-381.
4. Bacakova L, Filova E, Parizek M, et al. Modulation of cell adhesion, proliferation and differentiation on materials designed for body implants. *Biotechnol Adv*. 2011;29:739-767.
5. Kobayashi T, Nakamura S, Yamashita K. Enhanced osteobonding by negative surface charges of electrically polarized hydroxyapatite. *J Biomed Mater Res*. 2001;57:477-484.
6. Tarafder S, Bodhak S, Bandyopadhyay A, et al. Effect of electrical polarization and composition of biphasic calcium phosphates on early stage osteoblast interactions. *J Biomed Mater Res, Part B*. 2011;97B:306-314.
7. Yamashita K, Oikawa N, Umegaki T. Acceleration and deceleration of bone-like crystal growth on ceramic hydroxyapatite by electric poling. *Chem Mater*. 1996;8:2697-2700.
8. He J, Zhou W, Zhou X, et al. The anatase phase of nanotopography titania plays an important role on osteoblast cell morphology and proliferation. *J Mater Sci: Mater Med*. 2008;19:3465-3472.
9. Balint R, Cassidy NJ, Cartmell SH. Conductive polymers: towards a smart biomaterial for tissue engineering. *Acta Biomater*. 2014;10:2341-2353.
10. Ning C, Zhou L, Tan G. Fourth-generation biomedical materials. *Mater Today*. 2015;19:2-3.
11. Rajabi AH, Jaffe M, Arinzeh TL. Piezoelectric materials for tissue regeneration: a review. *Acta Biomater*. 2015;24:12-23.
12. Tofail SAM, Bauer J. Electrically polarized biomaterials. *Adv Mater*. 2016;28:5470-5484.
13. Childs PG, Boyle CA, Pemberton GD, et al. Use of nanoscale mechanical stimulation for control and manipulation of cell behaviour. *Acta Biomater*. 2016;34:159-168.
14. Jaffe B, Cook WR, Jaffe H. *Piezoelectric Ceramics*, 1st edn. India: Academic Press Limited; 1971.
15. Lyn PND. Lead toxicity, a review of the literature. Part I: exposure, evaluation, and treatment. *Altern Med Rev*. 2006;11:22.
16. Johnson FM. The genetic effects of environmental lead. *Mutat Res, Rev Mutat Res*. 1998;410:123-140.
17. García-Lestón J, Méndez J, Pásaro E, et al. Genotoxic effects of lead: an updated review. *Environ Int*. 2010;36:623-636.
18. Rödel J, Jo W, Seifert KTP, et al. Perspective on the development of lead-free piezoceramics. *J Am Ceram Soc*. 2009;92:1153-1177.
19. Rödel J, Webber KG, Dittmer R, et al. Transferring lead-free piezoelectric ceramics into application. *J Eur Ceram Soc*. 2015;35:1659-1681.
20. Takenaka T, Maruyama K-I, Sakata K. $Bi_{1/2}Na_{1/2}TiO_3$–$BaTiO_3$ system for lead-free piezoelectric applications. *Jpn J Appl Phys*. 1991;30:2236-2239.
21. Serfontein WJ, Mekel R, Bank S, et al. Bismuth toxicity in man - I. Bismuth blood and urine levels in patients after administration of a bismuth protein complex (Bicitropeptide). *Res Commun Chem Pathol Pharmacol*. 1979;26:383-389.
22. Rodilla V, Miles AT, Jenner W, et al. Exposure of cultured human proximal tubular cells to cadmium, mercury, zinc and bismuth: toxicity and metallothionein induction. *Chem-Biol Interact*. 1998;115:71-83.
23. Liu W, Ren X. Large piezoelectric effect in Pb-free ceramics. *Phys Rev Lett*. 2009;103:257602.
24. Yuan MM, Cheng L, Xu Q, et al. Biocompatible nanogenerators through high piezoelectric coefficient $0.5Ba(Zr_{0.2}Ti_{0.8})O_3$–$0.5(Ba_{0.7}Ca_{0.3})TiO_3$ nanowires for in-vivo applications. *Adv Mater*. 2014;26:7432-7437.
25. Scarisoreanu ND, Craciun F, Ion V, et al. Lead-free piezoelectric (Ba, Ca)(Zr, Ti)O_3 thin films for biocompatible and flexible devices. *ACS Appl Mater Interfaces*. 2017;9:266-278.
26. Li JF, Wang K, Zhu FY, et al. (K, Na)NbO_3-based lead-free piezoceramics: fundamental aspects, processing technologies, and remaining challenges. *J Am Ceram Soc*. 2013;96:3677-3696.
27. Malič B, Koruza J, Hreščak J, et al. Sintering of lead-free piezoelectric sodium potassium niobate ceramics. *Materials*. 2015;8:5449.
28. Yu S-W, Kuo S-T, Tuan W-H, et al. Ion release from three lead-free piezoelectric ceramics and their physical and cytotoxicity characteristics. *Mater Lett*. 2011;65:3522-3524.

29. Yu S-W, Kuo S-T, Tuan W-H, et al. Cytotoxicity and degradation behavior of potassium sodium niobate piezoelectric ceramics. *Ceram Int*. 2012;38:2845-2850.
30. Ayrikyan A, Rojas V, Molina-Luna L, et al. Enhancing electromechanical properties of lead-free ferroelectrics with bilayer ceramic/ceramic composites. *IEEE Trans Ultrason Ferroelectr Freq Control*. 2015;62:997-1006.
31. Acosta M, Novak N, Jo W, et al. Relationship between electromechanical properties and phase diagram in the $Ba(Zr_{0.2}Ti_{0.8})O_3$–$x(Ba_{0.7}Ca_{0.3})TiO_3$ lead-free piezoceramic. *Acta Mater*. 2014;80:48-55.
32. Vögler M, Acosta M, Brandt DRJ, et al. Temperature-dependent R-curve behavior of the lead-free ferroelectric $0.615Ba(Zr_{0.2}Ti_{0.8})O_3$–$0.385(Ba_{0.7}Ca_{0.3})TiO_3$ ceramic. *Eng Fract Mech*. 2015;144:68-77.
33. Ponsot I, Pontikes Y, Baldi G, et al. Magnetic glass ceramics by sintering of borosilicate glass and inorganic waste. *Materials*. 2014;7:5565-5580.
34. Lehnert D, Wehrle-Haller B, David C, et al. Cell behaviour on micropatterned substrata: limits of extracellular matrix geometry for spreading and adhesion. *J Cell Sci*. 2003;117:41.
35. Efe C, Yilmaz H, Tur YK, et al. Mechanical property characterization of $Na_1/2Bi_1/2TiO_3$–$BaTiO_3$ ceramics. *Int J Chem Eng Appl*. 2014;5:429-432.
36. Srinivas A, Krishnaiah RV, Niranjani VL, et al. Ferroelectric, piezoelectric and mechanical properties in lead free (0.5)Ba$(Zr_{0.2}Ti_{0.8})O_3$–(0.5)$(Ba_{0.7}Ca_{0.3})TiO_3$ electroceramics. *Ceram Int*. 2015;41:1980-1985.
37. Amaral M, Gomes PS, Lopes MA, et al. Cytotoxicity evaluation of nanocrystalline diamond coatings by fibroblast cell cultures. *Acta Biomater*. 2009;5:755-763.
38. Faucheux N, Schweiss R, Lutzow K, et al. Self-assembled monolayers with different terminating groups as model substrates for cell adhesion studies. *Biomaterials*. 2004;25:2721-2730.
39. Lee JH, Khang G, Lee JW, et al. Interaction of different types of cells on polymer surfaces with wettability gradient. *J Colloid Interface Sci*. 1998;205:323-330.
40. Dowling DP, Miller IS, Ardhaoui M, et al. Effect of surface wettability and topography on the adhesion of osteosarcoma cells on plasma-modified polystyrene. *J Biomater Appl*. 2010;26:327-347.
41. Xu L-C, Siedlecki CA. Effects of surface wettability and contact time on protein adhesion to biomaterial surfaces. *Biomaterials*. 2007;28:3273-3283.
42. Kosec M, Malic B, Wolny W, et al. Effect of achemically aggressive environment on the electromechanical behaviour ofmodified lead titanate ceramics. *J. Korean Phys. Soc*. 1998;32: S1163-S1166.
43. Foster WJ, Meen JK, Fox DA. The effect of physiologic aqueous solutions on the perovskite material lead-lanthanum-zirconium titanate (PLZT): potential retinotoxicity. *Cutan Ocul Toxicol*. 2013;32:18-22.
44. Bakarič T, Budič B, Malič B, et al. The influence of pH dependent ion leaching on the processing of lead-zirconate-titanate ceramics. *J Eur Ceram Soc*. 2015;35:2295-2302.
45. Jones JR. Review of bioactive glass: from Hench to hybrids. *Acta Biomater*. 2013;9:4457-4486.
46. Park N-G, Grätzel M, Miyasaka T, et al. Towards stable and commercially available perovskite solar cells. *Nat Energy*. 2016;1:16152.
47. Hailegnaw B, Kirmayer S, Edri E, et al. Rain on methylammonium lead iodide based perovskites: possible environmental effects of perovskite solar cells. *J Phys Chem Lett*. 2015;6:1543-1547.
48. Pollard TD, Earnshaw WC, Lippincott-Schwartz J. *Cell Biology, Easy Reading*. Saunders Elsevier, Philadelphia: Spektrum Akademischer Verlag; 2008.
49. Trevan JW. The error of determination of toxicity. *Proc R Soc Lond B Biol Sci*. 1927;101:483-513.
50. Sajin G, Petrescu D, Sajin M, et al. Interactions between biological media and piezoelectric ceramic in micromixing applications. *Rom J Inf Sci Tech Adv Mater*. 2007;10:279-289.
51. Sakai T, Hoshiai S, Nakamachi E. Biochemical compatibility of PZT piezoelectric ceramics covered with titanium thin film. *J Optoelectron Adv Mater*. 2006;8:1435-1437.
52. Yamamoto A, Honma R, Sumita M. Cytotoxicity evaluation of 43 metal salts using murine fibroblasts and osteoblastic cells. *J Biomed Mater Res*. 1998;39:331-340.
53. Hoppe A, Guldal NS, Boccaccini AR. A review of the biological response to ionic dissolution products from bioactive glasses and glass-ceramics. *Biomaterials*. 2011;32:2757-2774.
54. Bligh PH, Taylor DM. Comparative studies of metabolism of strontium and barium in rat. *Biochem J*. 1963;87:612-618.
55. Bodhak S, Bose S, Bandyopadhyay A. Role of surface charge and wettability on early stage mineralization and bone cell–materials interactions of polarized hydroxyapatite. *Acta Biomater*. 2009;5:2178-2188.
56. Horiuchi N, Nakaguki S, Wada N, et al. Polarization-induced surface charges in hydroxyapatite ceramics. *J Appl Phys*. 2014;116:014902.
57. Dames JE, Causton B, Bovell Y, et al. The migration of osteoblasts over substrata of discrete surface charge. *Biomaterials*. 1986;7:231-233.
58. Takeda H, Seki Y, Nakamura S, et al. Evaluation of electrical polarizability and in vitro bioactivity of apatite $Sr_5(PO_4)_3OH$ dense ceramics. *J Mater Chem*. 2002;12:2490-2495.

How to cite this article: Acosta M, Detsch R, Grünewald A, et al. Cytotoxicity, chemical stability, and surface properties of ferroelectric ceramics for biomaterials. *J Am Ceram Soc*. 2018;101:440–449. https://doi.org/10.1111/jace.15193